ACS APPLIED MATERIALS & INTERFACES

Research Article

www.acsami.org

Polymer/TiO_2 Hybrid Vesicles for Excellent UV Screening and Effective Encapsulation of Antioxidant Agents

Jianzhong Du* and Hui Sun

School of Materials Science and Engineering, Key Laboratory of Advanced Civil Engineering Materials of Ministry of Education, Tongji University 4800 Caoan Road, Shanghai, 201804, China

Supporting Information

ABSTRACT: Presented in this paper is a hybrid polymer/titanium dioxide (TiO_2) vesicle that has excellent UV-screening efficacy and strong capacity to encapsulate antioxidant agents. Poly(ethylene oxide)-*block*-poly(2-(dimethylamino)ethyl methacrylate)-*block*-polystyrene (PEO-*b*-PDMAEMA-*b*-PS) triblock terpolymer was synthesized by atom transfer radical polymerization (ATRP) and then self-assembled into vesicles. Those vesicles showed excellent UV-screening property due to the scattering by vesicles and the absorption by PS vesicle membrane. The selective deposition of solvophobic tetrabutyl titanate in the PDMAEMA shell and the PS membrane of the vesicles led to the formation of polymer/TiO_2 hybrid vesicles, resulting in an enhanced UV-screening property by further reflecting and scattering UV radiation. The vesicles can effectively encapsulate antioxidant agents such as ferulic acid (up to 57%), showing a rapid antioxidant capability (within 1 min) and a long-lasting antioxidant effect.

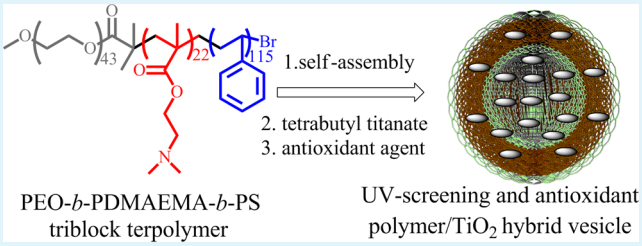

KEYWORDS: *triblock terpolymer, vesicle, titanium dioxide, UV screening, self-assembly, antioxidant agent*

1. INTRODUCTION

Exposure to UV rays may produce radicals, hurt human skin, and even cause certain skin cancers.[1−5] Therefore, UV-screening and antioxidant agents are essential ingredients in many skin care products. To effectively block UV radiation, both organic and inorganic materials had been developed based on different UV-screening mechanisms.[6,7] Organic polystyrene (PS) can absorb UV radiation, whereas inorganic TiO_2 can reflect and scatter UV light.[8] For example, we recently reported that the selective deposition of TiO_2 nanoparticles into the shell of a triblock terpolymer micelle provided a facile method for preparing TiO_2 nanoparticles with highly effective UV-screening activity but eliminated photocatalytic activity.[9] However, it is still an important challenge to develop a UV-screening material that can rapidly eliminate radicals and is also capable of long-time inhibition of radicals by retarded release of antioxidant agents.

Usually, hollow TiO_2 nanoparticles are obtained by sol−gel reactions using a *solid* template, which can be subsequently removed by either dissolution or calcinations.[10] However, the removal of the solid template is time- and cost-consuming. Polymer vesicles are hollow spheres that have endless applications in many fields.[11−19] To the best of our knowledge, using polymer vesicles as the template to prepare hollow TiO_2 nanoparticles has not been reported. The following are advantages of this strategy: (1) in situ formation of hollow nanoparticles with TiO_2 within the vesicle membrane, (2) no need to use organic solvents to remove the vesicle template, and (3) much less weight loss during the calcinations when preparing purely inorganic hollow TiO_2 nanoparticles.

In this paper, we first report the preparation of a triblock terpolymer vesicle that has excellent UV-screening activity (Scheme 1). Then, TiO_2 nanoparticles are deposited in situ in the vesicle membrane, forming hollow polymer/TiO_2 hybrid vesicles with enhanced UV-screening property (Scheme 1). Moreover, the polymer vesicles can encapsulate antioxidant agents such as ferulic acid (FA) with an ultrahigh loading efficiency. The FA-loaded vesicles exhibit long-term inhibition of radicals because of the sustained release of FA from the vesicles. Compared with our previous UV-screening polymer/TiO_2 hybrid micelles based on PEO_{43}-*b*-$PDMAEMA_{19}$-*b*-PS_{62} triblock terpolymer,[9] in this paper we will focus on the elimination of radicals by vesicles prepared from PEO_{43}-*b*-$PDMAEMA_{22}$-*b*-PS_{115} triblock terpolymer, which has a longer PS block.

2. RESULTS AND DISCUSSION

As shown in Scheme 1, the polymer/TiO_2 hybrid vesicles are prepared on the basis of the self-assembly of a poly(ethylene oxide)-*block*-poly(2-(dimethylamino)ethyl methacrylate)-*block*-polystyrene triblock terpolymer (PEO_{43}-*b*-$PDMAEMA_{22}$-*b*-PS_{115}) to form vesicle templates and the subsequent in situ sol−gel reactions. The polymer/TiO_2 hybrid vesicles are prepared in three steps: (1) PEO_{43}-*b*-$PDMAEMA_{22}$-*b*-PS_{115} triblock terpolymer is synthesized by atom transfer radical polymerization (ATRP), where the subscripts denote the mean

Received: May 1, 2014
Accepted: July 25, 2014
Published: July 25, 2014

Scheme 1. Preparation of UV-Screening and Antioxidant Polymer/TiO_2 Hybrid Vesicles[a]

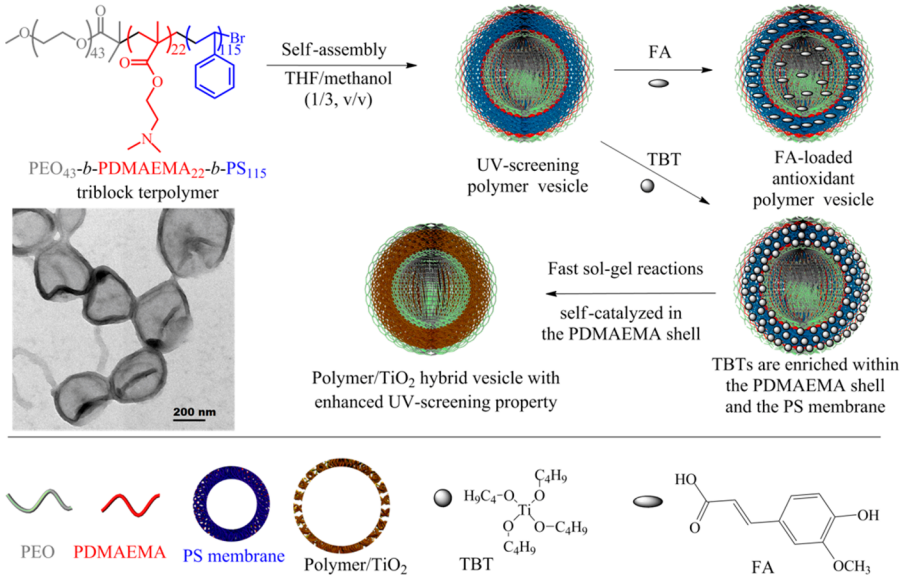

[a]PEO_{43}-*b*-$PDMAEMA_{22}$-*b*-PS_{115} triblock terpolymer self-assembles into vesicles in THF/methanol, which can effectively encapsulate antioxidant agents such as ferulic acid (FA). Furthermore, the solvophobic tetrabutyl titanate (TBT) can be enriched within the PDMAEMA shell and the PS membrane. Self-catalyzed fast sol−gel reaction in the PDMAEMA shell leads to a PDMAEMA/TiO_2 layer covered on the PS membrane, where subsequent slower sol−gel reaction leads to a PDMAEMA/PS/TiO_2 hybrid membrane. The hybrid vesicles possess enhanced UV-screening activity and can be further transformed to crystalline TiO_2 vesicles by calcinations. The hybrid vesicles can also encapsulate antioxidant FA with a very high loading efficiency.

degrees of polymerization of each block; (2) the triblock terpolymer is dissolved in THF and then a specific volume of methanol was added to induce the formation of polymer vesicles, with the solvophobic PS forming the membrane, the solvophilic PEO forming the outer corona, and the solvophilic PDMAEMA forming the middle shell; (3) The solvophobic tetrabutyl titanate (TBT) is added into the vesicles solution, which can be enriched in the solvophobic PS membrane and solvophilic PDMAEMA middle shell to form polymer/TiO_2 hybrid vesicles by PDMAEMA-catalyzed in situ sol−gel reactions. In addition, crystalline TiO_2 vesicles can be obtained by the subsequent calcinations of the hybrid vesicles.

2.1. Synthesis of PEO_{43}-*b*-$PDMAEMA_{22}$-*b*-PS_{115} Triblock Terpolymer. The PEO_{43}-*b*-$PDMAEMA_{22}$-*b*-PS_{115} triblock terpolymer was synthesized in two steps according to our previous ATRP protocol (see Scheme S1 in the Supporting Information).[9] The mean block composition of PEO_{43}-*b*-$PDMAEMA_{22}$-*b*-PS_{115} was determined by comparing the integrated areas of peaks b (PEO), f, h (PDMAEMA), and k (PS) in the ^{1}H NMR spectrum (Figure S1 in the Supporting Information). Both the ^{1}H NMR study and the GPC analysis (M_n = 21 000, M_w/M_n = 1.21, Figure S2 in the Supporting Information) confirmed the successful synthesis of this triblock terpolymer.

2.2. Self-Assembly of Triblock Terpolymer into Vesicles. Well-defined vesicles were formed spontaneously when methanol or water was added into the triblock terpolymer in THF at room temperature. PEO and PDMAEMA are soluble in methanol or water, while PS is insoluble. Thus, the PEO and PDMAEMA chains form the outer corona and the middle shell, while the insoluble PS chains form the membrane of the vesicle.

We studied the effects of the following three factors on the size and polydispersity (PDI) of polymer vesicles during the self-assembly: the volume ratio of the good solvent to the nonsolvent for PS (i.e., V_{THF} to $V_{methanol}$), the stirring rate, and the types of nonsolvent for PS (e.g., methanol and water).

When the volume ratio of THF to methanol was 1:2, the intensity-averaged hydrodynamic diameter (D_h) of vesicles was 277 nm with a very low PDI of 0.094, as determined by dynamic light scattering (DLS, see curve *a* in Figure 1). The size of vesicles increased to 303, 317, and 597 nm when more methanol was added into the polymer solution [see Figures 1 and S3 (Supporting Information)].

The stirring rate affects the size of polymer vesicles when either methanol (Figure 2) or water (Figure S4 in the Supporting Information) is used as the nonsolvent. When the stirring rates were 300, 450, and 600 rpm, the D_h values of

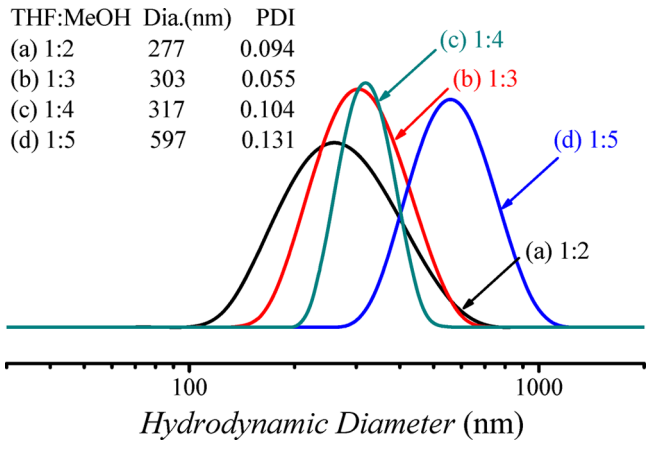

Figure 1. Intensity-averaged size distribution of polymer vesicles prepared at different volume ratios of THF/methanol. The stirring rate is fixed at 450 rpm. The DLS studies were performed in pure water (10 μL of vesicle solution was poured into 2 mL deionized water).

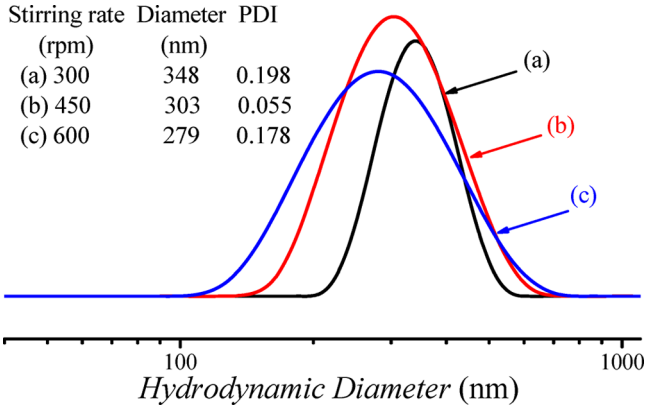

Figure 2. Intensity-averaged size distribution of vesicles at different stirring rates in THF/methanol (1:3). The DLS studies were performed in pure water.

polymer vesicles self-assembled in the mixture of THF/methanol were 348, 303, and 279 nm, respectively (Figure 2). The minimum size was obtained at 600 rpm, which was further confirmed by using water as the nonsolvent (Figure S4 in the Supporting Information).

At the same stirring rate and initial terpolymer concentration (2.0 mg/mL), more polar nonsolvent for PS such as water (compared with methanol) favors the formation of smaller vesicles. For example, at 450 rpm, the D_h values of polymer vesicles are 303 and 149 nm when using methanol and water as the nonsolvents, respectively. Moreover, the PDI in water is much less than that in methanol, indicating that the triblock terpolymer can form more uniform vesicles in water than in methanol. However, methanol is a much better solvent than water for the subsequent deposition of TiO_2 in the vesicle membrane, which will be discussed later.

2.3. Polymer/TiO_2 Hybrid Vesicles. The preparation conditions and DLS studies of the polymer/TiO_2 hybrid vesicles were summarized in Table S1 in the Supporting Information. DLS studies (curves b, c, d, and e in Figure 3) revealed that the D_h values of the hybrid vesicles were 310, 308, 287, and 300 nm by intensity (250, 273, 261, and 265 nm by number; Figure S5 in the Supporting Information) with very low PDIs when the molar ratios of DMAEMA:TBT was 1:0.5, 1:1, 1:1.5, and 1:2, respectively. Compared with the D_h of polymer vesicles without TiO_2, the addition of TBT did not change the structure of the precursor polymer vesicles. In addition, those polymer/TiO_2 hybrid vesicles can be redispersed in water for DLS characterizations and further applications (Figure S6 in the Supporting Information).

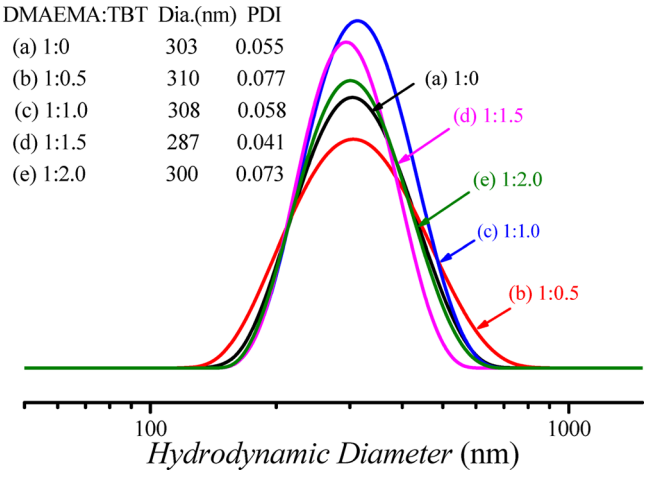

Figure 3. Intensity-averaged size distribution of triblock terpolymer vesicles at 0.5 mg/mL in methanol/THF by DLS before (a) and after (b–e) tetrabutyl titanate (TBT) deposition to form polymer/TiO_2 hybrid vesicles. The molar ratios of the DMAEMA unit to the TBT are (a) 1:0 (without TiO_2); (b) 1:0.5; (c) 1:1.0; (d) 1:1.5 and (e) 1:2.0, respectively. The DLS studies were performed in pure water.

The rate of sol–gel reactions of TBT to TiO_2 is faster in the PDMAEMA shell than that in the PS membrane because of the self-catalysis,[9] leading to a PDMAEMA/TiO_2 hybrid layer, which confined the unreacted solvophobic TBT molecules in the solvophobic PS membrane and then turned into titania upon further sol–gel reactions or calcinations.[9] As shown in the TEM images in Figure 4A,B, the number-averaged diameter in the TEM image is 230 ± 16 nm, which is reasonably slightly less than that by DLS (261 nm by number). More TEM images of the polymer/TiO_2 hybrid vesicles are shown in Figure S7 in the Supporting Information.

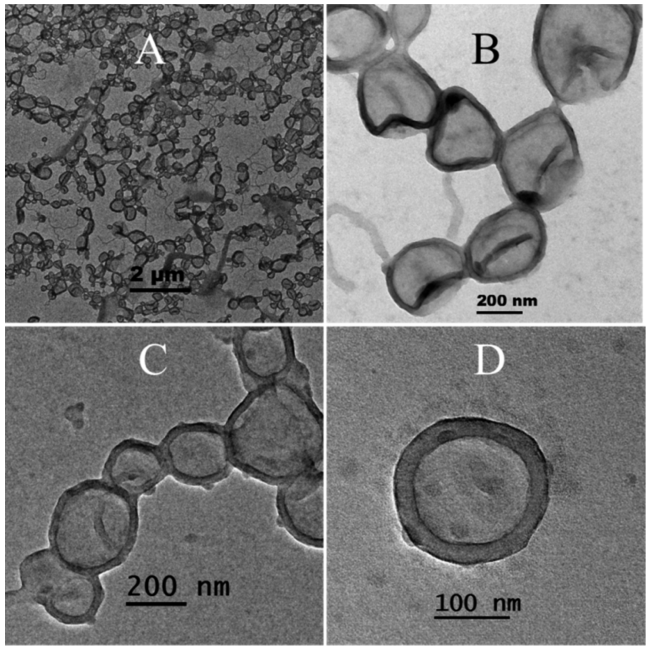

Figure 4. TEM images. (A and B) Polymer/TiO_2 hybrid vesicles before calcinations (DMAEMA/TBT is 1/1.5, n/n) with a diameter of 230 ± 16 nm. The thin dark layer (~25 nm) is PDMAEMA/PS/TiO_2 hybrid structure. (C and D) TiO_2 vesicles after calcinations with a diameter of 210 ± 20 nm.

In order to determine the stability of polymer/TiO_2 hybrid vesicles in various environments, the hybrid vesicles were redispersed in pure water at different pH values and evaluated by DLS (Figure S6 in the Supporting Information). At pH 2.0, 4.0, 6.0, 7.0, 8.0, 9.0, 10.0, and 11.0, the intensity-averaged D_h values are 233, 254, 231, 177, 209, 206, 216, and 210 nm, respectively. The corresponding number-averaged diameters are 173, 220, 195, 137, 176, 155, 164, and 165 nm with low PDI's, respectively. In general, this is consistent with the protonation at lower pH and deprotonation at higher pH of tertiary amine in the PDMAEMA shell of the vesicles, which has been further confirmed by the pH-dependent ζ-potential study (Figure S8, Supporting Information). Moreover, the

above results reveal that the TiO_2/polymer hybrid vesicles are stable at different pH values.

2.4. Hollow TiO_2 Vesicles. As shown in Figure 4C,D, TEM study confirmed the formation of TiO_2 vesicles after calcinations. TGA revealed 11% of solid residue (Figure S9 in the Supporting Information), coinciding with the theoretical value of 9.4%.

The number-averaged diameter of TiO_2 vesicles in the TEM image is 210 ± 20 nm, which is slightly smaller than the precursor hybrid vesicles, suggesting that the calcination of TiO_2/polymer hybrid vesicles leads to a slight shrinkage of vesicles. The thickness of the polymer/TiO_2 hybrid vesicles and inorganic TiO_2 vesicles is 25 ± 4 and 26 ± 3 nm, respectively. More importantly, the size of the TiO_2 vesicles can be tuned by controlling the sizes of the precursor polymer vesicles.

X-ray diffraction (XRD) pattern of inorganic TiO_2 vesicles in Figure 4C,D is shown in Figure 5. The sharp diffraction peaks

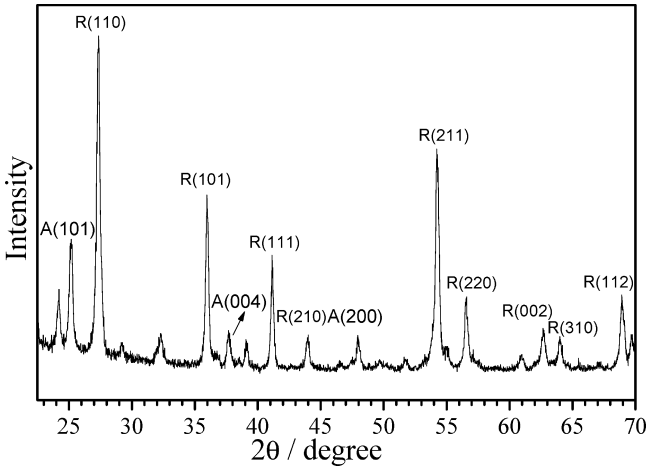

Figure 5. XRD pattern of rutile TiO_2 vesicles with a small amount of anatase.

indicated the majority as rutile phase and a small amount of anatase phase of TiO_2. In particular, the diffraction peaks at 2θ = 27.3°, 36.0°, 39.1°, 41.1°, 44.0°, 54.2°, 56.6°, 62.7°, 64.0°, and 69.0° are related to the (110), (101), (200), (111), (210), (211), (220), (002), (310), and (112) reticular planes of rutile.[20] The diffraction peaks at 2θ = 25.3° and 37.8° are related to the (101) and (004) reticular planes of anatase.[21]

To reveal the surface area and the porosity of TiO_2 vesicles, the nitrogen adsorption/desorption measurement was carried out by Brunauer–Emmett–Teller (BET) analysis, as shown in Figure 6. The isotherm was classified as type-IV and displayed a type-H3 hysteresis loop (IUPAC 13.2). The plot of pore size distribution was determined by the Barrett–Joyner–Halenda (BJH) method from the desorption branch of the isotherm, indicating the presence of mesoporous structure with an average diameter of 15.9 nm.[9] The specific surface area is 15.2 $m^2\ g^{-1}$ measured by BET. Nevertheless, the very low surface area suggests the poor photocatalytic activity of the TiO_2 vesicles.[9]

2.5. Comparison of ζ-Potentials among Purely Organic Polymer Vesicles, Polymer/TiO_2 Hybrid Vesicles, and TiO_2 Vesicles. In water, the ζ-potentials of the triblock terpolymer vesicles, polymer/TiO_2 hybrid vesicles (DMAEMA: TBT = 1:1.5, n/n), and TiO_2 nanoparticles, are +12.9, +7.88 and −27.5 mV, respectively. The positive charge

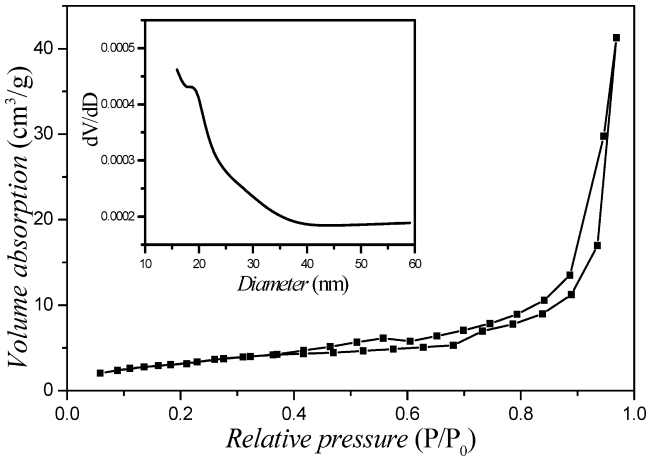

Figure 6. Nitrogen adsorption/desorption isotherm and corresponding pore size distribution curves of the TiO_2 vesicles.

(+12.9 mV) confirms the polymer vesicles having PEO coronas and PDMAEMA shells. The ζ-potential of polymer/TiO_2 hybrid vesicles was slightly decreased to +7.88 mV as a result of the electrostatic interaction and the hydrogen bonding formed between negatively charged TiO_2 vesicles and positively charged inner PDMAEMA shells. Also, it confirms the confined sol–gel reactions in the PDMAEMA shells and PS membranes, rather than the hydrophilic PEO coronas. Otherwise, a negative ζ-potential would be expected due to the surface-coated TiO_2. Actually, a negative charge (−27.5 mV) of TiO_2 vesicles is revealed as a result of calcinations, where the organic composition is burned off.

2.6. UV–Screening Property of Organic Polymer Vesicles and Organic/Inorganic Hybrid Vesicles. As shown in Figure 7, at the same concentration, the UV-transmittance at 245 nm of commercially available P25 TiO_2 (as control) reaches to 44.46, while the UV-transmittance of the organic polymer vesicles is as low as 1.358, indicating excellent UV-screening property of purely organic polymer vesicles. It is noteworthy that this is much better than that of

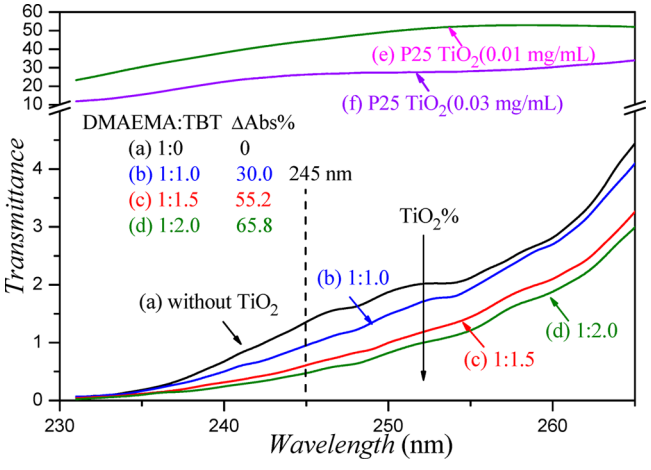

Figure 7. UV-transmittance spectra of polymer/TiO_2 hybrid vesicles (a–d) and commercially available P25 TiO_2 at 0.01 mg/mL (~10 ppm, e) and 0.03 mg/mL (f) in methanol. The molar ratios of the DMAEMA unit to TBT are (a) 1:0 (without TBT), (b) 1:1.0, (c) 1:1.5, and (d) 1:2.0, respectively.

our previously reported polymer micelles[9] because the bigger polymer vesicles can scatter more UV light than small micelles.

The UV-transmittance of hybrid vesicles at 230−265 nm wavelengths decreases with the feeding TBT, which is consistent with the excellent UVC (200−280 nm) shielding property of TiO_2.[22,23] Compared with the purely organic polymer vesicle, the UV-transmittance (e.g., at 245 nm) decreases by 30.0%, 55.2%, and 65.8% when the DMAEMA to TBT ratios are 1:1.0, 1:1.5, and 1:2.0, respectively, indicating the enhanced UV protection property of polymer/TiO_2 hybrid vesicles. The enhancement in the UV screening behavior is due to the strong reflection and scattering capability of TiO_2 nanoparticles against UV radiations. The overall UV-screening performance of hybrid vesicles is better than that of our previously reported hybrid micelles.[9]

2.7. Encapsulation of FA into Vesicles. The FA loading content (LC) of polymer vesicles is 25.6%.[24−32] The FA loading efficiency (LE) of this polymer vesicle is 51.9%, which is much higher than most of reported values for FA encapsulation.[18,33−38] For polymer/TiO_2 hybrid vesicles, the LC and LE are 28.7% and 57.4%, respectively.

The high loading content and loading efficiency of FA in the presence of vesicles (both before and after TBT deposition) are related to the poor solubility of FA in cold water. In the presence of vesicles, those FA molecules prefers to be accumulated into the hydrophobic vesicle membrane. Moreover, the electrostatic interaction between the amino groups in the vesicle shell and the carboxyl groups of FA molecules facilitates the encapsulation of FA. The ζ-potential of FA-loaded triblock terpolymer vesicles (without TBT deposition) is +18.6 mV, which is higher than that of the vesicles before FA loading (+12.9 mV), indicating the higher protonation degree of DMAEMA segments induced by FA.

2.8. Evaluation of the Antioxidant Effect of FA-Loaded Vesicles. The water-soluble 2,2′-azino-bis(3-ethylbenzothiazoline-6-sulfonic acid) diammonium salt (ABTS) radical is widely used in the evaluation of antioxidant effects. Figure 8 illustrates the relationship between the inhibition rates of FA at various concentrations against ABTS radical cation, confirming that the reaction between FA and ABTS radical cation is completed within 1 min. This is because some FA molecules adsorbed in the DMAEMA layer can react with ABTS radical cation immediately. Furthermore, more ABTS encapsulated in the cavity of the vesicles (ABTS "reservoir") can be diffused out through the vesicle membrane, resulting in a long time radical termination effect.

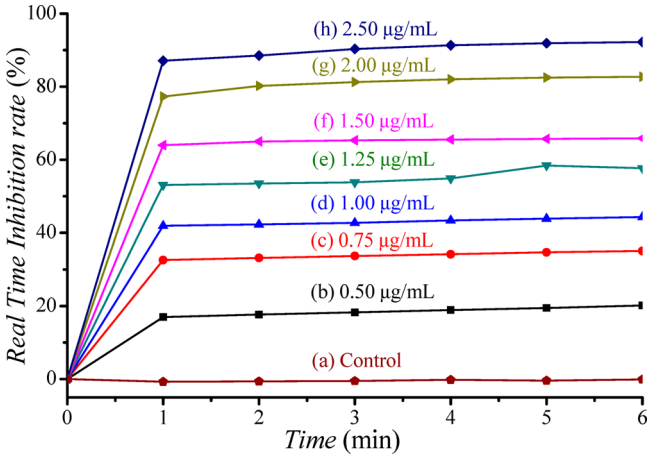

Figure 8. Relationship between the real time inhibition rates of ABTS radical cation at various FA concentrations.

When the concentration of FA reaches 2.5 μg/mL, the real time inhibition rate attains 90%, indicating the high antioxidant efficiency of FA-loaded vesicles (Figure 8). The relationship between the concentration of FA in the vesicle solutions and the real time inhibition rate of the ABTS radical cation is shown in Figure S10 in the Supporting Information.

Although ABTS radical cation is stable in aqueous solution (Figure 9b), it can be quickly inhibited by FA-encapsulated vesicles. For example, when mixed with a tiny amount of FA-loaded vesicles (1.0 μg/mL of FA), the inhibition rate was increased by 40% compared with the inhibition rate at the end of 1 min (Figure 9a). This also suggests the long-time and effective inhibition capacity of FA-loaded vesicles.

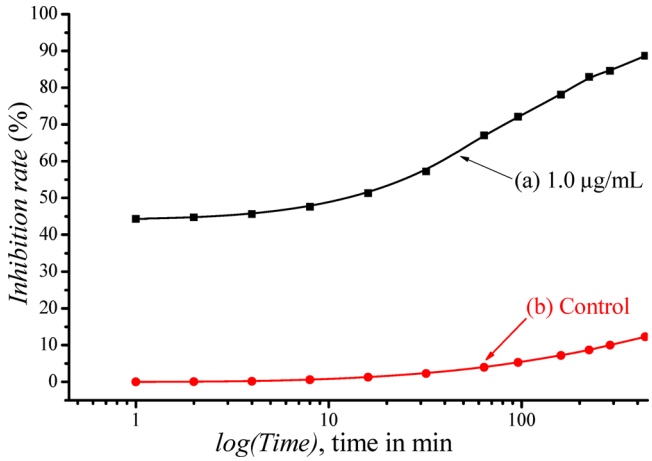

Figure 9. Long-time antioxidant activity of FA-loaded vesicles: (a) FA-loaded vesicles (1.0 μg/mL of FA) were mixed with ABTS radical cation and (b) only ABST radical cation.

3. EXPERIMENTAL SECTION

3.1. Materials. Poly(ethylene oxide) methyl ether (MeO−PEO−OH; M_n ca. 1900; M_w/M_n = 1.10) was purchased from Alfa Aesar and dried azeotropically using anhydrous toluene to remove traces of water. 2-(Dimethylamino)ethyl methacrylate (DMAEMA) was purchased from Sinopharm Chemical Reagent Co., Ltd. and passed through a silica gel column to remove inhibitor. 2-Bromoisobutyryl bromide, copper(I) bromide (CuBr, 99.999%), *N*,*N*,*N*′,*N*″,*N*″-pentamethyldiethylenetriamine (PMDETA, 98%), triethylamine, titanate precursor tetrabutyl titanate (TBT), Rhodamine B, *p*-xylene, ferulic acid (FA), tetrahydrofuran (THF), anhydrous ethanol, ABTS, anhydrous methanol (>99%, Beijing Chemical Reagent Co.), and other reagents were purchased from Aladdin Chemistry, Co. and used as received.

3.2. Characterization. The GPC, ^{1}H NMR, TEM, XRD, TGA, DLS, and BET analyses are performed under conditions similar to those of our previous work.[9]

ζ-Potential studies were conducted at 25 °C using a Zetasizer Nano ZS90 instrument (Malvern Instruments). The polymer/TiO_2 hybrid vesicles and inorganic TiO_2 vesicles were dispersed in deionized water at pH 6.05 and 6.14, respectively. No background electrolyte was added.

UV−vis studies were conducted using a UV−vis spectrophotometer (Shanghai Precision & Scientific Instrument Co., Ltd., UV759S) with a scan speed of 300 nm/min. The absorbance and transmittance spectra of the hybrid vesicles in the range of 200−265 nm wavelengths were recorded. The absorbance spectrum of the FA-loaded vesicles in the

range of 200−400 nm wavelengths was recorded, in which the absorbance at 323 nm was concerned. The antioxidant experiments were carried out by recording the absorbance at 734 nm of the mixed solution of the ABTS radical and FA-loaded vesicles.

3.3. Synthesis. The syntheses of PEO_{43}−Br macroinitiator and PEO_{43}-*b*-$PDMAEMA_{22}$-*b*-PS_{115} triblock terpolymer are similar to those of our previously published paper,[9] except that the polymerization time of styrene is 24 h and the yield of the terpolymer is 75% in this work.

3.4. Self-Assembly of Triblock Terpolymer into Vesicles. PEO_{43}-*b*-$PDMAEMA_{22}$-*b*-PS_{115} triblock terpolymer (10.0 mg) was dissolved in THF (5.0 mL). Different volumes of methanol (10.0, 15.0, 20.0, and 25.0 mL) were added dropwise at a constant stirring rate, respectively. Methanol or water (15 mL) was added dropwise at various stirring rates (300, 450, and 600 rpm), respectively.

3.5. Preparation of Polymer/TiO_2 Hybrid Vesicles and Inorganic TiO_2 Vesicles. The titanate precursor TBT (1.0 g) was first diluted in ethanol (10.0 g). In ample terpolymer vesicle solution (5.0 mL), TBT/ethanol with various molar ratios of DMAEMA to TBT was added under vigorous stirring for at least 24 h at room temperature. The initial concentration of polymer vesicles before the addition of TBT was 0.5 mg/mL in THF/methanol (1/3, v/v). The organic solvents were then removed by dialysis. The solution pH was adjusted by aqueous NaOH or HCl solution.

The inorganic TiO_2 vesicles were obtained by calcinations of the dried polymer/TiO_2 hybrid vesicles at 800 °C in a muffle for 3 h in air.

3.6. FA Loading of Vesicles. The triblock terpolymer (10.0 mg) and FA (5.0 mg) were dissolved in THF (5.0 mL). Deionized water (15 mL) was added dropwise in 50 min under continuous stirring. The unloaded FA was removed by dialysis against 2000 mL of deionized water at 25 °C for 2.5 h.[18] The water was renewed every 0.5 h.

The FA loading efficiency in the dialyzed vesicle solution was determined by a UV−vis spectrophotometer (UV-759S, Q/YXL270), comparing the absorbance of this solution at 323 nm with a calibration curve of the aqueous FA solution with known concentrations (Figure S11 in the Supporting Information). The final absorbance was calculated by subtracting the absorbance of the polymer at 323 nm at the same concentration. The FA loading content (LC) and FA loading efficiency (LE) were calculated according to the following eqs 1 and 2.[19]

$$\begin{aligned}\text{LC}\ (\%) &= (\text{weight of FA encapsulated in vesicles}) \\ &\quad /(\text{weight of polymer}) \times 100\% \\ &= (0.1124\ \text{mg/mL} \times 23.1\ \text{mL})/10.0\ \text{mg} \times 100\% \\ &= 25.6\% \end{aligned} \quad (1)$$

$$\begin{aligned}\text{LE}\ (\%) &= (\text{weight of FA encapsulated in vesicles}) \\ &\quad /(\text{weight of FA in feed}) \times 100\% \\ &= (0.1124\ \text{mg/mL} \times 23.1\ \text{mL})/5.0\ \text{mg} \times 100\% \\ &= 51.9\% \end{aligned} \quad (2)$$

3.7. Evaluation of the Scavenging Effect of FA-Loaded Vesicles on ABTS Radical Cation. The scavenging activity of FA-loaded vesicles against ABTS radical cation was evaluated according to published methods.[39,40] ABTS was dissolved in water (7.00 mM) and the radical cation solution was produced by reacting ABTS stock solution with potassium persulfate (2.45 mM of final concentration). The mixture was allowed to stand in the dark at room temperature for 12−16 h before use, resulting in the incomplete oxidation of ABTS because ABTS and potassium persulfate react stoichiometrically at a ratio of 1:0.5. After 6 h of oxidation, the absorbance of the solution reaches the maximum. The final concentration of the resulting green ABTS radical cation solution was adjusted to an absorbance of 0.900 ± 0.02 at 734 nm. The radical was stable in this form for more than 2 days when stored away from light at ambient temperature.

Then specific volumes of the FA-loaded vesicle solutions were mixed with 2.0 mL of ABTS radical cation solution obtained before, adjusting the whole volume to 3.0 mL with deionized water. The final FA concentrations were 0.5, 0.75, 1.0, 1.25, 1.5, 2.0, and 2.5 μg/mL, respectively. The absorbance at 734 nm of the mixture was recorded at the end of every minute within 6 min. The inhibition rate of FA radicals was calculated according to eq 3:

$$\text{inhibition rate}\ (\%) = (A_0 - A_1)/A_0 \times 100\% \quad (3)$$

where A_0 is the absorbance of ABTS solution and A_1 is the absorbance of the mixture.

3.8. Deposition of TBT into FA-Loaded Polymer Vesicles. The main procedure is the same as that in section 3.6. The molar ratio of TBT/DMAEMA is 1:2 and the TBT was added under vigorous stirring for at least 24 h at room temperature.

4. CONCLUSIONS

In conclusion, PEO_{43}-*b*-$PDMAEMA_{22}$-*b*-PS_{115} triblock terpolymer has been synthesized by ATRP and then self-assembled into vesicles with excellent UV-screening activity. Furthermore, the polymer vesicles have been used to mediate the formation of well-defined polymer/TiO_2 hybrid vesicles with better UV-screening property. Inorganic TiO_2 vesicles can be also prepared upon calcinations. Both organic and organic/inorganic hybrid vesicles can encapsulate antioxidant agents such as FA with very high loading content and loading efficiency. Moreover, the FA-loaded vesicles show a rapid antioxidant capability (within 1 min) and a long-lasting antioxidant effect. Overall, we have exploited a new strategy for preparing highly effective UV-screening polymer vesicles and polymer/TiO_2 hybrid vesicles with excellent antioxidant activity.

■ ASSOCIATED CONTENT

Supporting Information

Scheme S1, Figures S1−S11, and Table S1, which include characterizations of terpolymer, more DLS studies and TEM images of vesicles, TGA curve of hybrid vesicles, and a calibration curve of FA. This material is available free of charge via the Internet at http://pubs.acs.org.

■ AUTHOR INFORMATION

Corresponding Author

*Tel: +86-21-6958-0239. Fax: +86-21-6958-4723. E-mail: jzdu@tongji.edu.cn.

Notes

The authors declare no competing financial interest.

■ ACKNOWLEDGMENTS

J.D. is supported by Shanghai 1000 Plan, Eastern Scholar professorship, Ph.D. program foundation of Ministry of Education (20110072110048), Fok Ying Tong Education Foundation (132018), National Natural Science Foundation of China (21174107 and 21374080), and the Fundamental Research Funds for the Central Universities.

■ REFERENCES

(1) Habibi, M. H.; Nasr-Esfahani, M.; Emtiazi, G.; Hosseinkhani, B. Nanostructure Thin Films of Titanium Dioxide Coated on Glass and its Anti UV Effect for Living Organisms. *Curr. Nanosci.* **2010**, *6*, 324−329.

(2) Beasley, D. G.; Meyer, T. A. Characterization of the UVA Protection Provided by Avobenzone, Zinc Oxide, and Titanium Dioxide in Broad-Spectrum Sunscreen Products. *Am. J. Clin. Dermatol.* **2010**, *11*, 413−421.

(3) Meinke, M. C.; Friedrich, A.; Tscherch, K.; Haag, S. F.; Darvin, M. E.; Vollert, H.; Groth, N.; Lademann, J.; Rohn, S. Influence of Dietary Carotenoids on Radical Scavenging Capacity of the Skin and Skin Lipids. *Eur. J. Pharm. Biopharm.* **2013**, *84*, 365−373.
(4) Chen, C. Y. O.; Blumberg, J. B. In Vitro Activity of Almond Skin Polyphenols for Scavenging Free Radicals and Inducing Quinone Reductase. *J. Agric. Food Chem.* **2008**, *56*, 4427−4434.
(5) Herrling, T.; Fuchs, J.; Rehberg, J.; Groth, N. UV-induced Free Radicals in the Skin Detected by ESR Spectroscopy and Imaging Using Nitroxides. *Free Radical Biol. Med.* **2003**, *35*, 59−67.
(6) Sundarrajan, S.; Chandrasekaran, A. R.; Ramakrishna, S. An Update on Nanomaterials-Based Textiles for Protection and Decontamination. *J. Am. Ceram. Soc.* **2010**, *93*, 3955−3975.
(7) Montazer, M.; Pakdel, E.; Moghadam, M. B. Nano Titanium Dioxide on Wool Keratin as UV Absorber Stabilized by Butane Tetra Carboxylic Acid (BTCA): A Statistical Prospect. *Fibers Polym.* **2010**, *11*, 967−975.
(8) Dunford, R.; Salinaro, A.; Cai, L. Z.; Serpone, N.; Horikoshi, S.; Hidaka, H.; Knowland, J. Chemical Oxidation and DNA Damage Catalysed by Inorganic Sunscreen Ingredients. *FEBS Lett.* **1997**, *418*, 87−90.
(9) Xiao, J.; Chen, W. Q.; Wang, F. Y. K.; Du, J. Z. Polymer/TiO_2 Hybrid Nanoparticles with Highly Effective UV-Screening but Eliminated Photocatalytic Activity. *Macromolecules* **2013**, *46*, 375−383.
(10) Sasidharan, M.; Nakashima, K.; Gunawardhana, N.; Yokoi, T.; Inoue, M.; Yusa, S.; Yoshio, M.; Tatsumi, T. Novel Titania Hollow Nanospheres of Size 28 ± 1 nm Using Soft-Templates and Their Application for Lithium-Ion Rechargeable Batteries. *Chem. Commun.* **2011**, *47*, 6921−6923.
(11) Du, J. Z.; Chen, Y. M.; Zhang, Y. H.; Han, C. C.; Fischer, K.; Schmidt, M. Organic/Inorganic Hybrid Vesicles Based on a Reactive Block Copolymer. *J. Am. Chem. Soc.* **2003**, *125*, 14710−14711.
(12) Du, J. Z.; Armes, S. P. pH-Responsive Vesicles Based on a Hydrolytically Self-Cross-Linkable Copolymer. *J. Am. Chem. Soc.* **2005**, *127*, 12800−12801.
(13) Du, J. Z.; Chen, Y. M. Organic-Inorganic Hybrid Nanoparticles with a Complex Hollow Structure. *Angew. Chem., Int. Ed.* **2004**, *43*, 5084−5087.
(14) Zhou, C. C.; Wang, M. Z.; Zou, K. D.; Chen, J.; Zhu, Y. Q.; Du, J. Z. Antibacterial Polypeptide-Grafted Chitosan-Based Nanocapsules as an "Armed" Carrier of Anticancer and Antiepileptic Drugs. *ACS Macro Lett.* **2013**, *2*, 1021−1025.
(15) Chen, W. Q.; Du, J. Z. Ultrasound and pH Dually Responsive Polymer Vesicles for Anticancer Drug Delivery. *Sci. Rep.* **2013**, *3*, 2162.
(16) Zhu, Y. Q.; Wang, F. Y. K.; Zhang, C.; Du, J. Z. Preparation and Mechanism Insight of Nuclear Envelope-like Polymer Vesicles for Facile Loading of Biomacromolecules and Enhanced Biocatalytic Activity. *ACS Nano* **2014**, *8*, 6644−6654.
(17) Zhu, Y. Q.; Fan, L.; Yang, B.; Du, J. Z. Multifunctional Homopolymer Vesicles for Facile Immobilization of Gold Nanoparticles and Effective Water Remediation. *ACS Nano* **2014**, *8*, 5022−5031.
(18) Chen, M.; Liu, X.; Fahr, A. Skin Delivery of Ferulic Acid from Different Vesicular Systems. *J. Biomed. Nanotechnol.* **2010**, *6*, 577−585.
(19) Vianello, A.; Macri, F. NAD(P)H Oxidation Elicits Anion Superoxide Formation in Radish Plasmalemma Vesicles. *Biochim. Biophys. Acta* **1989**, *980*, 202−208.
(20) Bi, Y.; Ouyang, S.; Umezawa, N.; Cao, J.; Ye, J. Facet Effect of Single-Crystalline Ag_3PO_4 Sub-Microcrystals on Photocatalytic Properties. *J. Am. Chem. Soc.* **2011**, *133*, 6490−6492.
(21) Liu, Y. P.; Wang, S. R.; Shan, Z. Q.; Li, X. G.; Tian, J. H.; Mei, Y. M.; Ma, H. M.; Zhu, K. L. Anatase TiO_2 Hollow Spheres with Small Dimension Fabricated via a Simple Preparation Method for Dye-Sensitized Solar Cells with an Ionic Liquid Electrolyte. *Electrochim. Acta* **2012**, *60*, 422−427.
(22) Jiang, X.; Tian, X. Z.; Gu, J.; Huang, D.; Yang, Y. Q. Cotton Fabric Coated with Nano TiO_2−Acrylate Copolymer for Photocatalytic Self-Cleaning by in-Situ Suspension Polymerization. *Appl. Surf. Sci.* **2011**, *257*, 8451−8456.
(23) Asahi, R.; Morikawa, T.; Ohwaki, T.; Aoki, K.; Taga, Y. Visible-Light Photocatalysis in Nitrogen-Doped Titanium Oxides. *Science* **2001**, *293*, 269−271.
(24) Batrakova, E. V.; Kabanov, A. V. Pluronic Block Copolymers: Evolution of Drug Delivery Concept from Inert Nanocarriers to Biological Response Modifiers. *J. Controlled Release* **2008**, *130*, 98−106.
(25) Du, J. Z.; Fan, L.; Liu, Q. M. pH-Sensitive Block Copolymer Vesicles with Variable Trigger Points for Drug Delivery. *Macromolecules* **2012**, *45*, 8275−8283.
(26) Dufes, C.; Muller, J.-M.; Couet, W.; Olivier, J.-C.; Uchegbu, I. F.; Schätzlein, A. G. Anticancer Drug Delivery with Transferrin Targeted Polymeric Chitosan Vesicles. *Pharm. Res.* **2004**, *21*, 101−107.
(27) Fan, L.; Lu, H.; Zou, K. D.; Chen, J.; Du, J. Z. Homopolymer Vesicles with a Gradient Bilayer Membrane as Drug Carriers. *Chem. Commun.* **2013**, *49*, 11521−11523.
(28) Gabizon, A.; Shmeeda, H.; Horowitz, A. T.; Zalipsky, S. Tumor Cell Targeting of Liposome-Entrapped Drugs with Phospholipid-Anchored Folic Acid−PEG Conjugates. *Adv. Drug Delivery Rev.* **2004**, *56*, 1177−1192.
(29) Park, K. M.; Lee, D. W.; Sarkar, B.; Jung, H.; Kim, J.; Ko, Y. H.; Lee, K. E.; Jeon, H.; Kim, K. Reduction-Sensitive, Robust Vesicles with a Non-Covalently Modifiable Surface as a Multifunctional Drug-Delivery Platform. *Small* **2010**, *6*, 1430−1441.
(30) Ren, T. B.; Liu, Q. M.; Lu, H.; Liu, H. M.; Zhang, X.; Du, J. Z. Multifunctional Polymer Vesicles for Ultrasensitive Magnetic Resonance Imaging and Drug Delivery. *J. Mater. Chem.* **2012**, *22*, 12329.
(31) Upadhyay, K. K.; Bhatt, A. N.; Mishra, A. K.; Dwarakanath, B. S.; Jain, S.; Schatz, C.; Le Meins, J.-F.; Farooque, A.; Chandraiah, G.; Jain, A. K. The Intracellular Drug Delivery and Anti-Tumor Activity of Doxorubicin Loaded Poly(γ-benzyl L-glutamate)-*b*-hyaluronan Polymersomes. *Biomaterials* **2010**, *31*, 2882−2892.
(32) Yang, X.; Grailer, J. J.; Rowland, I. J.; Javadi, A.; Hurley, S. A.; Steeber, D. A.; Gong, S. Multifunctional SPIO/DOX-Loaded Worm-like Polymer Vesicles for Cancer Therapy and MR Imaging. *Biomaterials* **2010**, *31*, 9065−9073.
(33) Craparo, E. F.; Gennara, C.; Chiara, O. M.; Girolamo, T.; Luisa, B. M.; Gaetano, G. Amphiphilic Poly(hydroxyethylaspartamide) Derivative-Based Micelles as Drug Delivery Systems for Ferulic Acid. *J. Drug Targeting* **2009**, *17*, 78−88.
(34) Evans, K. O.; Harry-O'kuru, R. E. Antioxidation Behavior of Milkweed Oil 4-Hydroxy-3-methoxycinnamate Esters in Phospholipid Bilayers. *J. Am. Oil Chem. Soc.* **2013**, *90*, 1719−1727.
(35) Guo, T.; Sun, Y.; Sui, Y.; Li, F. M. Determination of Ferulic Acid and Adenosine in *Angelicae radix* by Micellar Electrokinetic Chromatography. *Anal. Bioanal. Chem.* **2003**, *375*, 840−843.
(36) Larsen, E.; Andreasen, M. F.; Christensen, L. P. Regioselective Dimerization of Ferulic Acid in a Micellar Solution. *J. Agric. Food Chem.* **2001**, *49*, 3471−3475.
(37) Laszlo, J. A.; Evans, K. O.; Vermillion, K. E.; Appell, M. Feruloyl Dioleoylglycerol Antioxidant Capacity in Phospholipid Vesicles. *J. Agric. Food Chem.* **2010**, *58*, 5842−5850.
(38) Manosroi, A.; Chutoprapat, R.; Abe, M.; Manosroi, W.; Manosroi, J. Anti-Aging Efficacy of Topical Formulations Containing Niosomes Entrapped with Rice Bran Bioactive Compounds. *Pharm. Biol.* **2012**, *50*, 208−224.
(39) Kim, D.-O.; Lee, K. W.; Lee, H. J.; Lee, C. Y. Vitamin C Equivalent Antioxidant Capacity (VCEAC) of Phenolic Phytochemicals. *J. Agric. Food Chem.* **2002**, *50*, 3713−3717.
(40) Re, R.; Pellegrini, N.; Proteggente, A.; Pannala, A.; Yang, M.; Rice-Evans, C. Antioxidant Activity Applying an Improved ABTS Radical Cation Decolorization Assay. *Free Radical Biol. Med.* **1999**, *26*, 1231−1237.